Korean J. Chem. Eng., **27**(3), 962-969 (2010)
DOI: 10.1007/s11814-010-0152-4

Adsorption of carbon dioxide onto BDA-CP-MS41

Youngson Choe*, Kwang-Joong Oh*, Seong-Soo Kim, and Sang-Wook Park*,†**

*Division of Chemical Engineering, Pusan National University, Busan 609-735, Korea
**School of Environmental Science, Catholic University of Pusan, Busan 609-757, Korea
(*Received 14 September 2009 • accepted 2 November 2009*)

Abstract−Carbon dioxide was adsorbed onto mesoporous adsorbent of butylene diamine immobilized CP-MS41 (BDA-CP-MS41), which was synthesized by chloropropyl functionalized MCM-41 (CP-MS41) with butylene diamine in a laboratory-scale packed-bed. The adsorber was operated batchwise with the charge of adsorbent in the range of 1-3 g to obtain the breakthrough curves of CO_2. Experiments were carried out at different adsorption temperatures (20-40 °C) and flow rates of nitrogen (10-20 cm^3/min) to investigate the effects of these experimental variables on the breakthrough curves. The deactivation model was tested for these curves by combining the adsorption of CO_2 and the deactivation of adsorbent particles. The observed values of the adsorption rate constant and the deactivation rate constant were evaluated through analysis of the experimental breakthrough data using a nonlinear least squares technique. The experimental breakthrough data fitted very well to the deactivation model than the adsorption isotherm models in the literature.

Key words: Adsorption, Carbon Dioxide, Breakthrough Curve, Deactivation Model, Mesoporous Adsorbent

INTRODUCTION

Carbon dioxide (CO_2) produced by combustion of fossil fuels is regarded as the most significant greenhouse gas with its increasing accumulation in the atmosphere attracting worldwide attention [1]. Various methods have been used to remove it: absorption by solvent and adsorption by molecular sieve, membrane separation, and cryogenic fractionation. In particular, absorption has been widely used in the chemical industries, as with the Benfield Process [2]. Another technique is dry scrubbing or sorption of CO_2 onto an alkaline metal carbonate as a solid adsorbent. This is a modified hybrid technology of adsorption and chemical absorption, with the advantage of being a simple and convenient operation for separation and recovery of CO_2 in flue gases. The development of alkaline metal carbonates, such as an alumina gel [3], alumina [4], activated carbon [5-7], and silica/alumina vermiculite [8], is the focus of the current study to improve the sorption efficiency of the carbonate. Adsorption is one of the most widely employed methods in practical industrial operation because of the easy operation and low cost with efficient recovery of the solute [9]. The most important characteristics of porous adsorbents are their surface properties such as porous structure, pore size distribution, wall thickness, specific surface area, and hydrophilic-hydrophobic properties. The discovery of the M41S family by a Mobil scientist [10,11] generated a great deal of interest in the synthesis of organically-functionalized, mesoporous materials for their application in the fields of catalysis, sensing, and adsorption, given their high surface areas and large ordered pores ranging from 20 to 100 Å [11,12] with narrow size distributions. High chemical and thermal stabilities also make them potential and promising candidates for the reactions of bulky substrate molecules. In general, hybrid organic-inorganic materials have been prepared *via* post-grafting or co-condensation techniques. In 2000, Bhaumik and Tatsumi [13] reported a grafting technique through a co-condensation method for hybrid MCM-41 using halogenated organosilanes. Recently, a new synthetic approach has been developed for the preparation of hybrid inorganic-organic mesoporous materials based on the co-condensation of siloxane and organosiloxane precursors in the presence of different templating surfactant solutions [14-17]. Huang and Yang [18] reported the sorption-reaction mechanism between CO_2 and a functional group of NH_2 attached in the adsorbent of 3-aminopropyltriethoxysilane - immobilized ionic liquid on MCM-46, and they presented the reaction of CO_2 onto the adsorbent. Xu et al. [19] used polyethyleneimine - immobilized adsorbent on MCM-41. Ju et al. [20] reported a new grafting technique for the synthesis of hybrid MCM-41 and trialkylamine-immobilized ionic liquids containing high catalytic activity for the synthesis of cyclic carbonates from CO_2. In the case of MCM-41 containing a functional group of amine, CO_2 can be adsorbed like CO_2 absorption in alkanolamines. Park et al. have immobilized ethylene diamine [21] and propylene diamine [22] on hybrid MCM-41 to adsorb CO_2, respectively. They presented that the ethylene group had higher adsorption capacity than propylene.

In mass transfer processes that accompany chemical reactions, such as a non-catalytic heterogeneous gas-solid reaction [23-27], the diffusion may have an effect on the reaction kinetics [28]. It is difficult and tedious to analyze the adsorption breakthrough curve using conventional isotherm models [29,30], such as the Langmuir, Freundlich, Brunauer-Emmett-Teller (BET), and Dubinin-Radushkevich-Kagener (DRK) models, and prepare the experimental values of the sorption isotherm with a reasonable diffusivity [31] of a solute. Conversely, the deactivation model (DM) [32,33], as a simplified model, has been used to predict the breakthrough curve, assuming that the formation of a dense product layer over the surface

†To whom correspondence should be addressed.
E-mail: swpark@pusan.ac.kr

of the adsorbent changed the number of active sites and the possible variations in the adsorption of active sites to cause a drop in the adsorption rate. Suyadal et al. [34] presented adsorption kinetics of trichloroethylene vapor on activated carbon using breakthrough curves by DM and assumed that the adsorption kinetics of DM were first-order with respect to organic vapor and zeroth order with respect to activity of the adsorbent, respectively, but, not first-order with respect to activity of the adsorbent. Park et al. have successfully applied DM for carbonation of sodium carbonate [35], potassium carbonate [36] with CO_2, and adsorption of toluene vapor [37], and VOCs [38] onto activated carbon. They have indicated DM described gas-solid non-catalytic reactions more accurately than the unreacted core and volume reaction models, using deactivation kinetics with first-order with respect to the solid carbonate and the CO_2 concentration, respectively.

To our knowledge, no literature report about CO_2 adsorption using amine immobilized has yet been published except the articles as mentioned above [18,19,21,22]. In this study, the solid particle of butylene diamine - immobilized ionic liquid (BDA-CP-MS41) on the hybrid CP-MS41, synthesized in the previous work [20], was used as an adsorbent of CO_2, which is one of the series of works [21,22,35-38] to investigate the adsorption kinetics from analysis of the breakthrough data by DM and to present the relationship between the breakthrough data and the adsorption isotherm, and to compare its capacity with those of other alkyl diamines [21,22].

THEORY

The formation of a dense product layer over the solid adsorbent creates an additional diffusion resistance and is expected to cause a drop in the adsorption rate. One would also expect it to cause significant changes in the accessible pore volume, active surface area, and activity per unit area of solid adsorbent with respect to the extent of the adsorption. All of these changes cause a decrease of vacant surface area of the adsorbent with time. In DM, the effects of all of these factors on the diminishing rate of CO_2 capture are combined in a deactivation rate term.

With assumptions [38] of the pseudo-steady state and the isothermal species, the conservation equation for CO_2 in the fixed bed is

$$-Q_o\frac{dC_A}{dS}-k_oC_A\alpha=0 \tag{1}$$

In writing this equation, axial dispersion in the fixed bed and any mass transfer resistances are assumed to be negligible. According to the proposed DM, the rate of change of the activity of the solid adsorbent is expressed as

$$-\frac{d\alpha}{dt}=k_dC_A^n\alpha^m \tag{2}$$

The zeroth solution of the deactivation models is obtained by taking n=0. m=1, and the initial activity of the solid as unity.

$$a=\exp[-k_o\tau\exp(-k_dt)] \tag{3}$$

Eq. (3) is identical to the breakthrough equation proposed by Suyadal et al. [34] and assumes a fluid phase concentration that is independent of deactivation processes along the adsorber. More realistically, one would expect the deactivation rate to be concentration dependent and, accordingly, axial-position-dependent in the fixed bed.

To obtain the analytical solution of Eq. (1) and (2) by taking n=m=1, an iterative procedure is applied. The procedure used here is similar to the paper proposed by Dogu [39] for the approximate solution of nonlinear equations. In this paper, the zeroth solution (Eq. (3)) is substituted into Eq. (2), and the first correction for the activity is obtained by the integration of this equation. Then, the corrected activity expression is substituted into Eq. (1), and integration of this equation gives the first corrected solution for the breakthrough curve.

$$a=\exp\left[\frac{[1-\exp(k_o\tau(1-\exp(-k_dt)))]}{1-\exp(-k_dt)}\exp(-k_dt)\right] \tag{4}$$

This iterative procedure can be repeated for further improvement of the solution. In this procedure, higher-order terms in the series solutions of the integrals are neglected. The breakthrough curve for the deactivation model with two parameters (k_ot and k_d) is calculated from the concentration profiles by Eq. (4).

EXPERIMENTAL

1. Chemicals

All chemicals were of reagent grade and were used without further purification. Purity of both CO_2 and N_2 was greater than 99.9%. Butylene diamine (BDA), tetraethylorthosilicate (TEOS), 3-chloropropyltriethoxysilane (CITPES), cetyltrimethylammonium bromide (CTMABr), and tetramethylammounium hydroxide were supplied by Aldrich chemical company, U.S.A.

2. Synthesis of BDA-CP-MS41

CP-MS41 was synthesized by hydrolysis of TEOS, as a silicon source, with CITPES as an organosilane using CTMABr as a template. PDA-CP-MS41 was synthesized by immobilization of BDA on the mesoporous CP-MS41. Both synthetic procedures of CP-MS41 and BDA-CP-MS41 followed previous work [20], where the measured values of the surface area by BET isotherm, particle size by SEM, pore diameter by N_2 adsorption using BjH method, and micropore surface and micropore volume by t-plot method of CP-MS41 were 884.6 m^2/g, 5.0 μm, 28 Å, 105 m^2/g, and 0.06 cm^3/g, respectively. The bed porosity of the fixed bed was measured by a conventional method [40] using a mass cylinder and its value was 0.76.

3. An Apparatus for CO_2 Capture and its Operation

An adsorption experiment (Fig. 1) was carried out in the presence of CO_2 with BDA-CP-MS41 adsorbent in a fixed bed pyrex glass reactor with internal diameter of 2 cm. CO_2 was carried by nitrogen gas through a sparger. The concentration of CO_2 in the nitrogen stream at the outlet of the sparger was measured by a gas chromatograph. The flow rate of the gas mixture of CO_2 and nitrogen was within the range of 10-20 cm^3/min (measured at 25 °C). The amount of adsorbent and the adsorption temperature were in the range of 1-3 g, 20-40 °C, respectively. Experiments were repeated three times to obtain the average value for each type of experiment. A gas chromatograph (detector: thermal conductivity detector; column: Haysep D (10 feet by 1/8 inch of stainless steel; detector temperature: 190 °C; feed temperature: 160 °C; flow rate of He: 25.7 cm^3/min; retention time of N_2, CO_2: 1.497, 2.08 min, respectively.) connected to the exit stream of the adsorber allowed for on-line analysis of CO_2 and N_2.

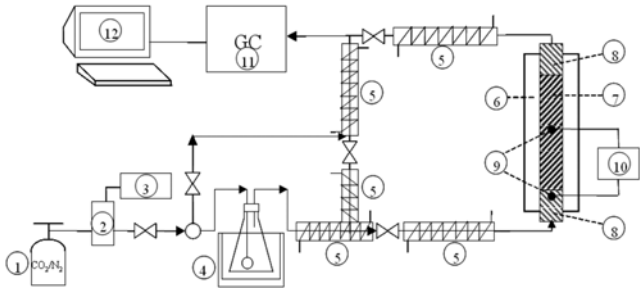

Fig. 1. Schematic diagram of a fixed bed apparatus.

1. Gas bomb
2. Mass flow controller
3. Flow indicator
4. Saturator
5. Heating line
6. Furnace
7. Sample
8. Glass wool
9. Temperature probe
10. Temperature controller
11. GC (gas chromatography)
12. Personal computer

BDA-CP-MS41 particles were supported by glass wool from both sides. The adsorber was placed into a tubular furnace equipped with a temperature controller. The length of the fixed adsorbent section of the bed was 5 cm of the adsorber. Temperature profiles were not observed within this section. All of the flow lines between the adsorber and the gas analyzer were heated to eliminate any condensation. Three-way valves placed before and after the adsorber allowed for flow of the gaseous mixture through the bypass line during flow rate adjustments. Composition of the inlet stream was checked by the analysis of the stream flowing through the bypass line at the start experiments. The experimental procedure used to obtain the breakthrough curve of CO_2 was identical as that reported in detail previously [22].

RESULTS AND DISCUSSION

1. FTIR Study of CO_2 Adsorption

The surface interaction of CO_2 with the amine-modified samples (BDA-CP-MS41) was studied using infrared spectroscopy. Strong IR bands were observed in the range of 1,700-1,300 cm^{-1}; adsorbed gaseous CO_2, bicarbonate in C-O bending, carbamate in C-O bending, and NH_3^+.

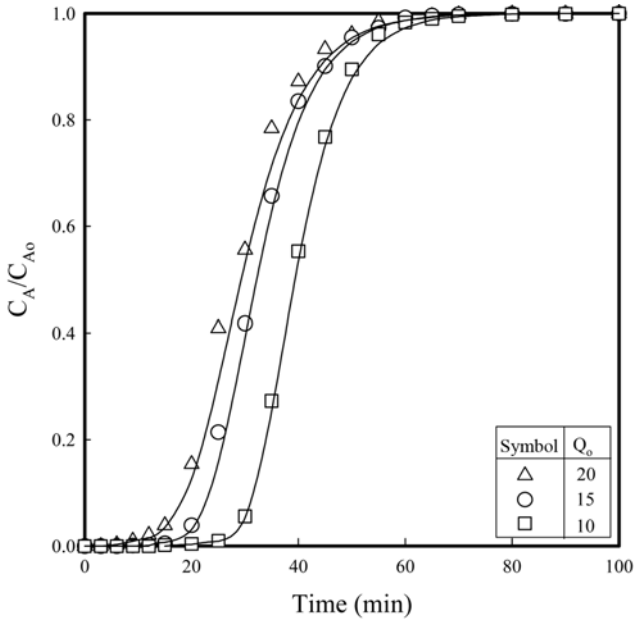

Fig. 2. Effect of flow rates of gaseous mixtures on the breakthrough curve of CO_2 (y_A=0.15, W=2 g; T=30 °C).

2. Kinetics of CO_2 Adsorption on BDA-CP-MS41

To investigate the adsorption kinetics of CO_2 on BDA-CP-MS41 using two parameters of DM, the breakthrough curves of CO_2 were measured according to changes of the experimental variables such as flow rate of carrier gas, amount of adsorbent, and adsorption temperature.

3. Effect of Flow Rate of Gaseous Mixtures of CO_2 and N_2

To investigate the effect of flow rate of gaseous mixtures of CO_2 and N_2 on the kinetics, the breakthrough curves of CO_2 were measured in the range of flow rate of gaseous mixtures from 10-20 cm^3/

Table 1. Rate parameters for various experimental conditions

T (°C)	Q_o (cm^3/min)	W (g)	y_A (-)	$k_o\tau$ (-)	$k_o \times 10^8$ (m/min)	k_d (m^3/kmol·min)	r^2 (-)
30	10	2	0.15	5.866	3.309	0.158	0.999
30	15	2	0.15	4.346	3.677	0.145	0.999
30	15	2	0.15	6.748*	5.710*	0.106*	0.996
30	20	2	0.15	3.408	3.845	0.132	0.997
30	15	1.5	0.15	3.351	3.781	1.137	0.994
30	15	2	0.15	4.346	3.677	0.145	0.999
30	15	3	0.15	5.802	3.273	0.153	0.994
30	15	2	0.05	4.085	3.456	0.132	0.993
30	15	2	0.15	4.346	3.677	0.145	0.999
30	15	2	0.50	4.607	3.898	0.158	0.991
20	15	2	0.15	3.366	2.848	0.039	0.995
25	15	2	0.15	3.923	3.319	0.078	0.991
30	15	2	0.15	4.346	3.677	0.145	0.999
40	15	2	0.15	6.694	5.664	0.537	0.993

The asterisk symbol (*) means adsorption with moisture

min (measured at 25 °C) under the typical experimental conditions such as 15% of CO_2 concentration, 30 °C and 2 g of the adsorbent. The measured outlet concentrations of CO_2 were typically plotted against the adsorption time for the various flow rates indicated as various symbols in Fig. 2.

As shown in Fig. 2, a shift of breakthrough curves to shorter times was observed at greater flow rate of the gaseous mixture with decrease in the amount of CO_2 that the bed can hold up to a certain breakthrough level. This result means that the adsorbed amount of CO_2 decreases as the space time of the gaseous mixtures in the fixed bed decreases. The breakthrough curve was evaluated by analysis of the experimental breakthrough data using a nonlinear least squares technique with the parameters of $k_o\tau$, k_o and k_d (tabulated in Table 1, and drawn as a solid line in Fig. 2). As shown in Fig. 2, the regression analysis of the experimental breakthrough data gave very good agreement with the breakthrough equation Eq. (4) with regression coefficient more than 0.999. As shown in Table 1, the values of $k_o\tau$ decreased with increasing Q_o where the k_o's and k_d's were almost same.

4. Effect of Amount of BDA-CP-MS41

A set of experiments was performed to investigate the effect of the mass of BDA-CP-MS41 in the range from 1 to 3 g on the CO_2 breakthrough curves. As shown in Fig. 3, a good description of data was obtained by using Eq. (4) for each set of amount of BDA-CP-MS41 at y_A of 0.15, T of 30 °C, and Q_o of 15 cm^3/min.

Also, the adsorbed amount of CO_2 increased with increasing the amount of BDA-CP-MS41. The model parameters determined from the analysis of the experimental breakthrough data are tabulated in Table 1. As shown in Table 1, the values of $k_o\tau$ increase with increasing W, whereas the k_o's and k_d's are almost same.

5. Effect of Feedstock Concentration of CO_2

To determine the dependence of the adsorption parameters on the feedstock concentration of CO_2, the breakthrough curves of CO_2 were measured in the range of CO_2 concentration from 5-50% at flow rate of the gaseous mixture of 15 cm^3/min, temperature of 30 °C, and BDA-CP-MS41 of 2 g. A good fitting of DM predictions to experimental data could be seen by inserting the corresponding values of $k_o\tau$ and k_d tabulated in Table 1 into Eq. (4), which were almost same. The calculated breakthrough curve (solid line) of CO_2 with the mean values of $k_o\tau$ and k_d and measured ones (various symbols) is shown in Fig. 4. As shown in Fig. 4, the measured values approached to the calculated value with correlation coefficient of 0.9988 and mean deviation of 0.0225. This result comes from independence of the concentration of CO_2 on the breakthrough curves

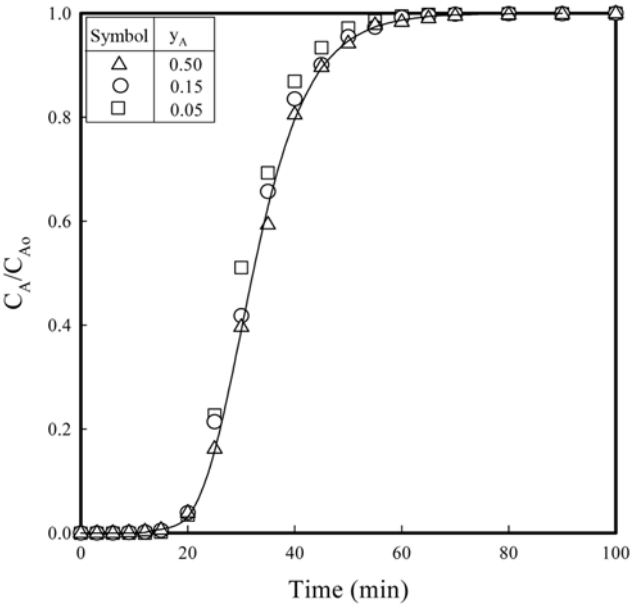

Fig. 4. Effect of CO_2 concentration on the breakthrough curve of CO_2 (Q_o=15 cm^3/min, W=2 g, T=30 °C).

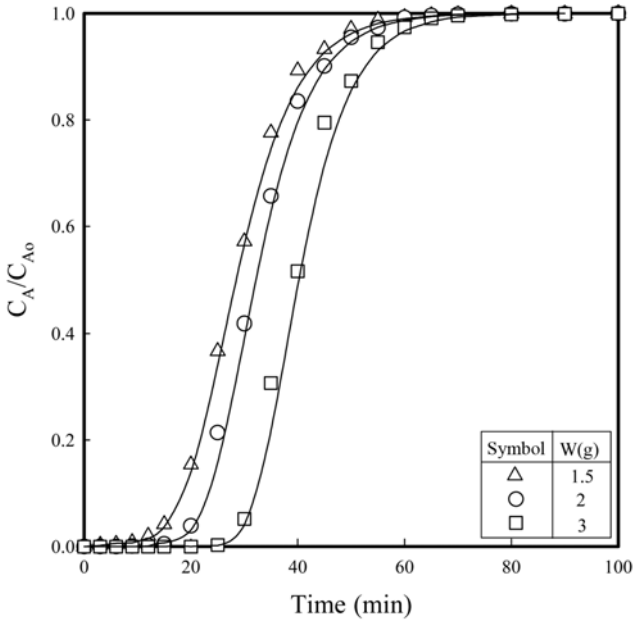

Fig. 3. Effect of amount of adsorbent on the breakthrough curve of CO_2 (Q_o=15 cm^3/min, y_A=0.15, T=30 °C).

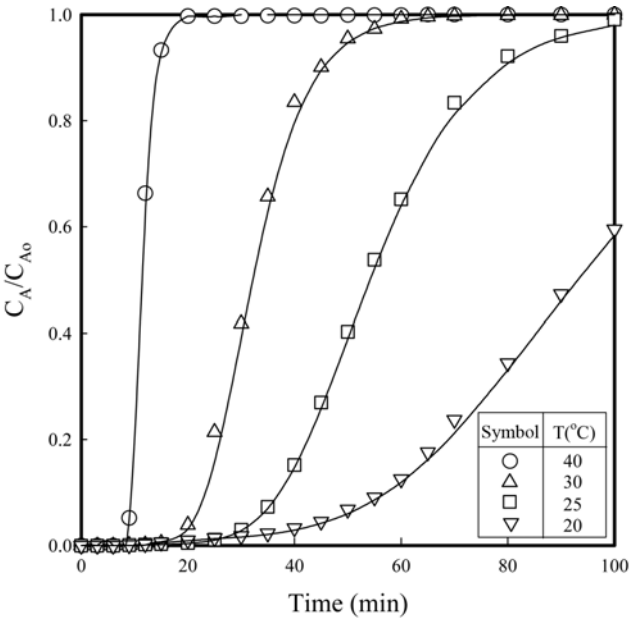

Fig. 5. Effect of adsorption temperature on the breakthrough curve of CO_2 (Q_o=15 cm^3/min, W=2 g, T=30 °C).

of CO_2 as shown in Eq. (4).

6. Effect of Adsorption Temperature

To investigate the effect of adsorption temperature on the adsorption kinetics, the breakthrough curves of CO_2 were measured in the range of temperature from 20-40 °C. The measured outlet concentrations of CO_2 were typically plotted against the adsorption time for the various temperatures indicated as various symbols in Fig. 5 under the typical experimental conditions of 55 m^3/min of the gaseous mixture and 2 g of BDA-CP-MS41. The model parameters were evaluated by analysis of the experimental breakthrough data using a nonlinear least squares technique and are tabulated in Table 1. The results in Fig. 5 indicated a shift in breakthrough curves toward the left with increased temperature, which might be attributed to an increase in the amount of adsorbed CO_2 due to increase of reaction and deactivation and was the same result of the breakthrough curves of trichloroethylene vapor on EDA (ethylene diamine)-CP-MS41 [34]. Arrhenius plots of k_o and k_d are shown in Fig. 6. The activation energy for the adsorption (ΔE_a) and deactivation (ΔE_d) was obtained from the slopes of plots in Fig. 6, and their values were 22.3 and 99.8 kJ/mole, respectively.

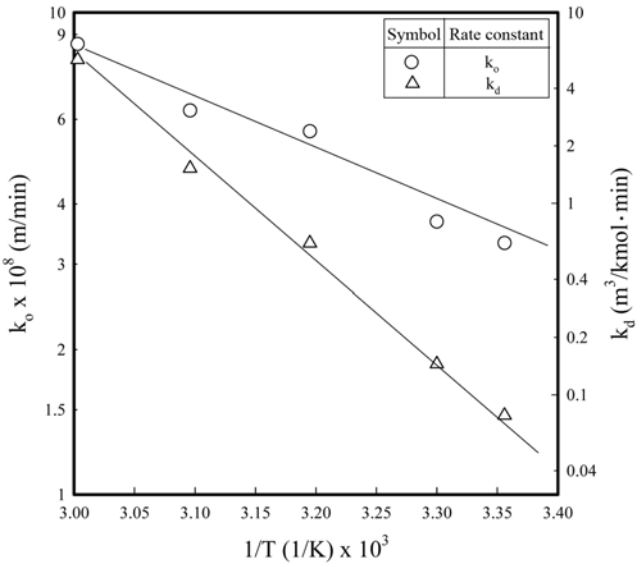

Fig. 6. Effect of adsorption temperature on dimensionless absorption rate constant and deactivation rate constant.

7. Adsorption Accompanied with Chemical Reaction

Huang and Yang [18] and Leal et al. [41] presented the chemical reaction mechanism between CO_2 and the amine-immobilized-MCM48 and amine-immobilized-3-aminopropyltriethoxysilane, respectively, where the adsorption of CO_2 onto the solid particles with and without moisture is as follows:

IR bands were complicatedly observed in the range of 1,700-1,300 cm^{-1};

They presented FTIR such as adsorbed gaseous CO_2 (1,330 cm^{-1}), bicarbonate in C-O bending (1,382 cm^{-1}), carbamate in C-O bending (1,432 and 1,485 cm^{-1}), and NH_3^+ (1,560 and 1,635 cm^{-1}), formed by the reaction CO_2 and -NH_2 without water and with water, respectively. Also, from TGA analysis, the presence of water moisture doubled the amount of CO_2 adsorbed. In this study, the FTIR spectrum, as mentioned in the section of FTIR study of CO_2 adsorption, confirmed the same results. The breakthrough curves of CO_2 were measured at CO_2 concentration of 15%, the flow rate of the gaseous mixture of 15 cm^3/min, temperature of 30 °C, and BDA-CP-MS41 of 2 g with and without water moisture in Fig. 8.

As shown in Fig. 8, the breakthrough curve shifts toward the right with water moisture, and $k_o\tau$ and k_d, tabulated in Table 1, were 6.748 and 0.106 m^3/kmol·min, respectively. This $k_o\tau$ was larger than that without moisture and the k_d, smaller than that without moisture. The upper area of the breakthrough curve of CO_2 was integrated according to the adsorption stream time to evaluate the weight change of CO_2, which is shown in Fig. 9. The amount of CO_2 adsorbed with moisture was 184.46 mg/g-adsorbent, which was 89.2% larger than 97.47 mg/g-adsorbent during 140 minutes. It might be experimental error that the adsorbed CO_2 was not double.

To observe the effect of alkylene group in immobilized alkylene

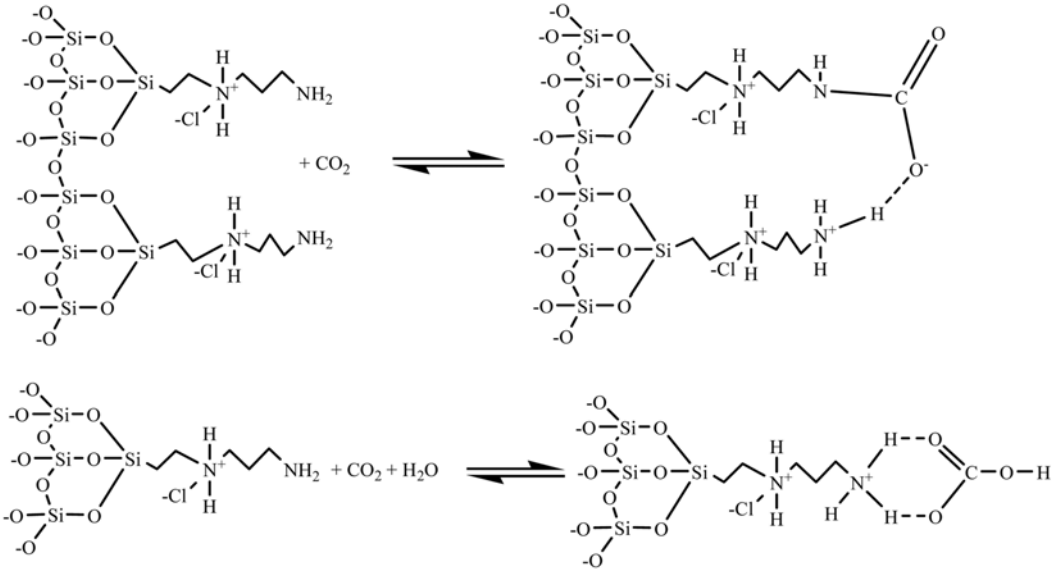

Fig. 7. Surface reaction mechanism of CO_2 without and with moisture for adsorption of CO_2 onto BDA-CP-MS41.

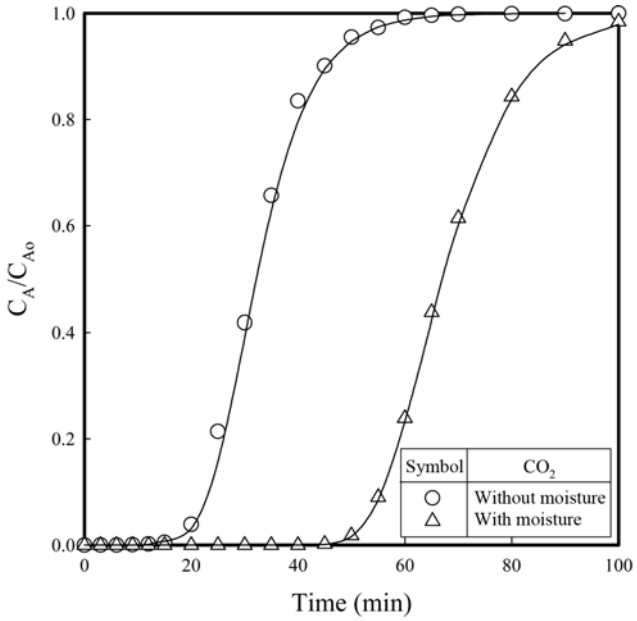

Fig. 8. Effect of moisture on the breakthrough curve of CO_2 (Q_o= 15 cm^3/min, y_A=0.15, W=2 g, T=30 °C).

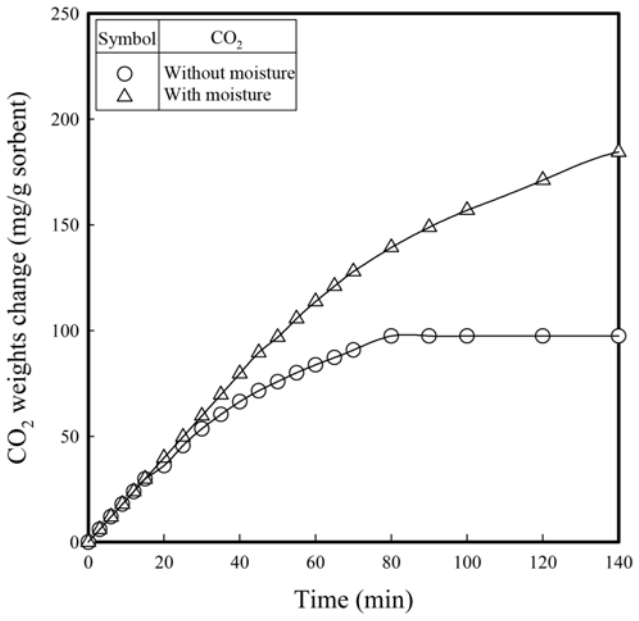

Fig. 9. Amount of CO_2 adsorbed with/without moisture under the same experimental conditions in Fig. 8.

diamine on the adsorption capacity, the values of k_o, k_d, ΔE_a, ΔE_d, and adsorbed amount of CO_2 for ethylene, propylene, and butylene group were used. These values for the typical conditions of T=30 °C, Q_o=15 cm^3/min, W=2 g, y_A=0.15, and adsorption time=100 min are listed in Table 3. The data for ethylene and propylene were cited in the previous works [21,22]. As shown in Table 3, k_d, ΔE_a, and ΔE_d, increase and k_o and adsorbed amount of CO_2 decrease in ethylene, propylene, and butylenes order, which means that the shorter the length of alkyl group, the larger the adsorption capacity of CO_2, assuming alkyl group with short length group moves more easily and has more chance to meet CO_2 than long size.

8. Comparison of the Proposed Models

Several equilibrium models [30], which have been developed to describe adsorption isotherm relationships, are useful for describing adsorption capacity and theoretical evaluation of thermodynamic parameters, such as heats of adsorption. But sometimes the experimental procedure to prepare the adsorption isotherm relationships is very tedious and time consuming. The equilibrium concentrations between two phases, which are used to describe adsorption isotherm relationships, can be obtained by Eq. (5) and (6), where a(t), x and y are the dimensionless concentrations of CO_2 in the breakthrough data (42), in the gas phase and solid phase, respectively.

$$x = \frac{\int_0^t a(t)dt}{\int_0^\infty a(t)dt} \tag{5}$$

Table 2. Selected adsorption isotherms to fit the breakthrough data of CO_2 for comparison with the deactivation model

Adsorption isotherms	Mathematical representation of adsorption isotherms	Linearized forms	Parameters and correlation coefficient
Langmuir	$y = \frac{ax}{(1+bx)}$	$\frac{1}{y} = \frac{1}{ax} + \frac{b}{a}$	a=259.7 b=268.4 r^2=0.8880
Freundlich	$y=ax^b$	$\ln(y)=\ln(a)+b\ln(x)$	a=1.0981 b=0.2192 r^2=0.9469
Brunauer-Emmett-Teller	$y = \frac{x}{(1-x)(a+bx)}$	$\frac{x}{y(1-x)} = a+bx$	a=−0.3532 b=5.6562 r^2=0.6057
Dubinin-Radshkevich-Kagener	$y=a\exp[-b\ln^2(x)]$	$\ln(y)=\ln(a)-b\ln^2(x)$	a=0.5776 b=0.0247 r^2=0.6885
Deactivation model (this study)	x according to Eq. (5) y according to Eq. (6)		$k_S\tau$=4.346 k_d=0.145 r^2=0.99929

Table 3. Effect of alkylene group on adsorption capacity of CO_2

Alkylene diamine	$k_o \times 10^8$ (m/min)	k_d (m^3/kmol·min)	ΔE_a (kJ/mol)	ΔE_d (kJ/mol)	Adsorbed CO_2 (mg/g)
Ethylene diamine [21]	6.151	0.074	16.2	96.7	298
Propylene diamine [22]	5.716	0.113	20.2	98.0	185
Butylene diamine (this study)	3.309	0.158	22.3	99.8	97

Adsorption conditions; T=30 °C, Q_o=15 cm^3/min, W=2 g, y_A=0.15, time=100 min

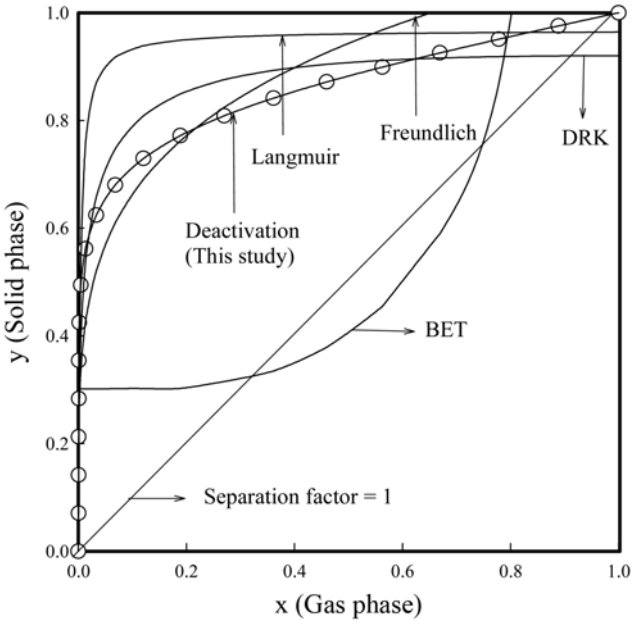

Fig. 10. Comparison of the model in describing the experimental breakthrough curve of CO_2 according to Table 2 under the same experimental conditions in Fig. 8.

$$y = \frac{t - x\int_0^\infty a(t)dt}{\int_0^\infty dt - \int_0^\infty a(t)dt} \quad (6)$$

As shown in Eqs. (5) and (6), the ranges of x and y are between 0 and 1, respectively. The equilibriums for single-solute sorption given in the literature [30] are frequently presented as dimensionless concentration isotherms. To compare the deactivation model with the equilibrium isotherm models, models selected by Suyadal et al. [34] were used as follows: Langmuir, Freundlich, BET, and DRK model, whose formulas are listed in Table 2. The typical experimental conditions indicated as circles were used, i.e., gaseous flow rate of 15 cm^3/min, amounts of BDA-CP-MS41, 2 g, and adsorption temperature, 30 °C. Using a(t) obtained from the experimental parameters, the values of x and y obtained from Eq. (5) and (6), are shown in Fig. 10 and used to obtain the constants of a and b in each model.

As shown in Table 2 and Fig. 10, the proposed deactivation model fitted the data with the highest correlation (r^2) of 0.9999, and the adsorption of CO_2 on BDA-CP-MS41 might be favorable isotherms due to the separation factor less than unity. Failure of BET, Langmuir, DRK, and Freundlich model in order in the fitting with the experimental data in Fig. 10 may be explained by the gas-solid heterogeneous reaction containing adsorption between CO_2 and BDA-CP-MS41.

CONCLUSIONS

Mesoporous BDA-CP-MS41 was used as an adsorbent to capture CO_2 and the breakthrough data were measured in a fixed bed to observe the adsorption kinetics. The adsorption kinetics was assumed to be the first-order with respect to the concentration of CO_2 and the activity of the adsorbent, respectively. The adsorption and deactivation rate constant were evaluated by the deactivation model through analysis of the experimental breakthrough data using a nonlinear least squares technique. Moisture actually increased the CO_2 adsorption capacity because of the special chemical reaction mechanism between CO_2 and amines in BDA-CP-MS41. The experimental breakthrough data fitted very well to the deactivation model than the adsorption isotherm models in the literature. As compared with the size of the alkylene group in immobilized alkylene diamine, the adsorption capacity of CO_2 increased in ethylene, propylene, and butylenes order.

ACKNOWLEDGMENTS

This work was supported by Korea Ministry of Environment (MOE) as Human resource development Project for Waste to Energy, a grant (2006CCD11P011A-21-3-010) from Energy Technology R&D of the Korea Energy Management Corporation, and the National Research Foundation of Korea Grant founded by the Korean Government (NRF-2009-K20601000004-00410).

NOMENCLATURE

a : ratio of outlet concentration of CO_2 to inlet concentration
C_A : concentration of CO_2 in gaseous stream
k_d : deactivation rate constant [m^3/kmol·min]
k_o : adsorption rate constant [m/min]
m : deactivation order in Eq. (2)
n : adsorption order in Eq. (2)
Q_o : flow rate of gaseous mixtures of N_2 and CO_2 [m^3/min]
r^2 : correlation coefficient
S : surface area of adsorbent [m^2]
t : adsorption time [min]
T : adsorption temperature [K]
x : dimensionless concentrations of CO_2 in the gas phase through the sorption isotherm
y : dimensionless concentrations of CO_2 in the solid phase through the sorption isotherm
V_G : volume of gas in the absorber [m^3]
y_A : mole fraction of CO_2

W : amount of adsorbent [g]

Greek Letters

α : activity of the solid adsorbent

τ : surface-time defined as ratio of S to Q_o [min/m]

Subscripts

A : CO_2

o : inlet

REFERENCES

1. M. Aresta, *Carbon dioxide recovery and utilization*, Kluwer academic Pub., Boston (2003).
2. R. K. Bartoo, *Chem. Eng. Prog*., **80**, 35 (1984).
3. W. Fuchs and N. T. Syosett, U.S. Patent 3,511,595 (1970).
4. D. Gidaspow and M. Onischak, U.S. Patent 3,865,924 (1975).
5. S. Hirano, N. Shigomoto, S. Yamada and H. Hayashi, *Bull. Chem. Soc., Jpn*., **68**, 1030 (1995).
6. H. Hayashi, H. J. Taniuchi, N. Furuyashiki, S. Sugiyama, S. Hirano, N. Shigemoto and T. Nonaka, *Ind. Eng. Chem. Res*., **37**, 185 (1998).
7. T. Shigemoto, S. Sugiyama and H. Hayashi, *J. Chem. Eng. Jpn*., **38**, 711 (2005).
8. A. G. Okunev, V. E. Sharnov, Y. I. Aristov and V. N. Parmon, *React. Kinet. Catal. Lett*., **71**, 355 (2004).
9. M. L. Ruhl, *Chem. Eng. Prog*., **89**, 1344 (1993).
10. C. T. Kresge, M. E. Leonowicz, W. J. Roth, J. C. Vartuli and J. S. Beck, *Nature*, **359**, 710 (1992).
11. J. S. Beck, J. C. Vartuli, W. J. Roth, M. E. Leonowicz, C. T. Kresge, K. D. Schmitt, C. T. W. Chu, D. H. Olson, E. W. Sheppard, S. B. McCullen, J. B. Higgins and J. L. Schlenker, *J. Am. Chem. Soc*., **114**, 10834 (1992).
12. D. Zhao, J. Feng, Q. Huo, N. Melosh, G. H. Fredrickson, B. F. Chmelka and G. D. Stucky, *Science*, **279**, 548 (1998).
13. A. Bhaumik and T. Tatsumi, *J. Catal*., **189**, 31 (2000).
14. S. L. Burkett, S. D. Sim and S. J. Mann, *J. Chem. Soc. Chem. Commun*., 1367 (1996).
15. M. H. Lim, C. F. Blanford and A. Stein, *J. Am. Chem. Soc*., **119**, 4090 (1997).
16. C. E. Fowler, B. Lebeau and S. Mann, *J. Chem. Soc. Chem. Commun*., 1825 (1998).
17. F. Babonneau, L. Leite and S. Fontlupt, *J. Mater. Chem*., **9**, 175 (1999).
18. H. Y. Huang and R. T. Yang, *Ind. Eng. Chem. Res*., **42**, 2427 (2003).
19. X. Xu, C. Song, B. G. Miller and A. W. Scaroni, *Fuel Proc. Technol*., **86**, 1457 (2005).
20. H. Y. Ju, K. H. Kim and D. W. Park, *Korean J. Chem. Eng.*, **27**, 446 (2010).
21. K. S. Hwang, Y. S. Son, S. W. Park, D. W. Park, K. J. Oh and S. S. Kim, *Sep. Sci. Technol*., **45**, 85 (2010).
22. K. S. Hwang, L. Han, D. W. Park, K. J. Oh, S. S. Kim and S. W. Park, *Korean J. Chem. Eng*., **27**, 241 (2010).
23. L. K. Doraiswamy and M. M. Sharma, *Heterogeneous reactions*, John Wiley & Sons, New York (1954).
24. M. Ishida and C. Y. Wen, *AIChE J*., **14**, 311 (1968).
25. P. A. Pamachandran and B. D. Kulkarni, *Ind. Eng. Chem. Res. Process Des. Dev*., **19**, 717 (1980).
26. J. W. Evans and S. Song, *Ind. Eng. Chem. Process Des. Dev*., **13**, 146 (1974).
27. B. S. Sampath, P. A. Ramachandran and R. Hughes, *Chem. Eng. Sci*., **30**, 135 (1975).
28. M. G. Ranade and J. W. Evans, *Ind. Eng. Chem. Process Des. Dev*., **19**, 118 (1980).
29. D. M. Ruthven, *Principles of adsorption and adsorption processes*, John & Wiley, New York (1984).
30. M. Suzuki, *Adsorption engineering*, Kodansga Ltd., Tokyo (1990).
31. N. Orbey, G. Dogu and T. Dogu, *Can. J. Chem. Eng*., **60**, 314 (1982).
32. S. Yasyerli, T. Dogu, G. Dogu and I. Ar, *Chem. Eng. Sci.*, **51**, 2523 (1996).
33. T. Kopac and S. Kocabas, *Chem. Eng. Comm*., **190**, 1041 (2003).
34. Y. Suyadal, M. Erol and M. Oguz, *Ind. Eng. Chem. Res*., **39**, 724 (2000).
35. S. W. Park, D. W. Sung, B. S. Choi and K. W. Oh, *Sep. Sci. Technol*., **41**, 2665 (2006).
36. S. W. Park, D. W. Sung, B. S. Choi, J. W. Lee and H. Kumazawa, *J. Ind. Eng. Chem*.,**12**, 522 (2006).
37. S. W. Park, B. S. Choi and J. W. Lee, *Sep. Sci. Technol*., **42**, 2221 (2007).
38. K. S. Hwang, D. W. Kim, S. W. Park, D. W. Park, K. J. Oh and S. S. Kim, *Korean J. Chem. Eng*., **27**, 632 (2010).
39. T. Dogu, *AIChE J*., **32**, 849 (1986).
40. K. S. Hwang, S. W. Park, D. W. Park, K. J. Oh and S. S. Kim, *Korean J. Chem. Eng*., **26**, 1383 (2009).
41. O. Leal, C. Bolivar, C. Ovalles, J. J. Garcia and Y. Espidel, *Inorganica Chimica Acta*, **240**, 183 (1995).
42. S. Yasyerli, G. Dogu and I. Ar, *Chem. Eng. Comm*., **190**, 1055 (2003).